Detrending Moving Average Algorithm: a brief review

Anna Carbone
Physics Department Politecnico di Torino,
Corso Duca degli Abruzzi 24, I-10129 Torino, Italy
anna.carbone@polito.it
http://www.polito.it/noiselab

***Abstract*—A short review of an algorithm, called Detrending Moving Average, to estimate the Hurst exponent H of fractals with arbitrary dimension is presented. Therefore, it has the ability to quantify temporal and spatial long-range dependence of fractal sets. Moreover, the method, in addition to accomplish accurate and fast estimates of H, can provide interesting clues between fractal properties, self-organized criticality and entropy of long-range correlated fractal sets.**

I. Introduction

Thanks to Internet-based connectivity and communication technologies, millions of individual interactions among people can be recorded and are available for investigation. Hence, high-volume and high-quality data can be analysed by means of robust techniques, originally developed within more traditional areas of statistical physics and complexity. Algorithms for quantifying the concepts of scaling, criticality, self-similarity, only to cite a few examples, are currently adopted in the framework of technological and social science investigation [1]–[13]. Size and scales of social and economic phenomena are changing due to the way collective human interactions presently occur. Social phenomena emerge and develop under the effect and action of components, whose dynamics is influenced by the increased amount of interactions and information exchange through large numbers of heterogeneous agents. The common idea is that elementary components of the system through their interaction spontaneously develop collective behaviors that could not have been deduced on the basis of simple additivity. Time series are a tool to describe social and economic systems in one dimension, such as stock market indexes and exchange rates [14]–[22]. Extended systems evolving over space, such as urban textures, world wide web and firms are described in terms of random structures in high-dimensional representation. Firm size, income, words frequency, financial indexes are distributed according to *power laws*, since they evolve under the effect of *correlations* typical of physical systems with a large number of interacting units. The extreme complexity of modern communication and computer networks, coupled with their traffic characteristics - heavy tails, self-similarity and long-range dependence - makes the characterization of their performance through analytical models an extremely difficult task [23]–[25]. Under such circumstances, simulations become one of the most promising tools for understanding the behavior of such systems. The application of fractal concepts, through the estimate of H, has been proven useful in a variety of fields. Fractal behavior and long-range dependence have been observed in an astonishing number of physical, biological and socio-economic systems. Time series, profiles and surfaces can be characterized by the fractal dimension D, a measure of roughness, and by the Hurst exponent H, a measure of long-memory dependence. The assumption of statistical self-affinity implies a linear relationship between fractal dimension and Hurst exponent and thereby links the two phenomena through the embedded dimension d. For example in $d = 1$, heartbeat intervals of healthy and sick hearts are discriminated on the basis of the value of H [26], [27]; different stages of financial market development are related to the correlation degree of return and volatility series [17]; coding and non coding regions of genomic sequences have different Hurst exponent [28]; climate models are checked against long-term correlated atmospheric and oceanographic series [29], [30]. In $d \geq 2$ fractal measures are used to model and quantify stress induced morphological transformation [31]; isotropic and anisotropic fracture surfaces [32]–[36]; static friction between materials dominated by hard core interactions [37]; diffusion [38], [39] and transport [40], [41] in porous and composite materials; mass fractal features in wet/dried gels [42] and in physiological organs (e.g. lung) [43]; hydrophobicity of surfaces with hierarchic structure undergoing natural selection mechanism [44] and solubility of nanoparticles [45]; digital elevation models [46] and slope fits of planetary surfaces [47].

A number of methods aimed at quantifying long-range dependence have been proposed to accomplish accurate and fast estimates of H in order to investigate correlations at different scales. This work reviews the main properties of an algorithm, called Detrending Moving Average (DMA), for estimating the Hurst exponent of fractals with arbitrary dimension [49]–[59].

II. Fractional Brownian and Levy Motions

One of the simplest models exhibiting long-range dependence is fractional Brownian motion (fBm) introduced by Kolmogorov and further developed by Mandelbrot and Van Ness [48]. It is a Gaussian, non-stationary, self-similar pro-

978-1-4244-3878-5/09/$25.00 ©2009 IEEE

cess indexed by a parameter H. The self-similar nature of fBm is particularly relevant for simulating financial markets, growing firms, queueing networks only to cite a few examples. However, several long range correlated processes do not show an agreement with the assumption of Gaussian marginal distribution valid for fractional Brownian motion. There exists empirical evidence supporting a heavy tailed assumption backed by theoretical work that explains how the former assumption induces through an appropriate mechanism long-range dependence in many systems. Therefore, a more general process that exhibits in a natural way both scaling behavior and heavy tails should be considered. Levy motions or Levy processes are a class of random functions, which are a natural generalization of the Brownian motion and whose increments are stationary, statistically self-affine and stably distributed according to Levy. The ordinary Levy motions generalize the ordinary Brownian motions, with independent increments. The fractional Levy motions generalize the fractional Brownian motions, with interdependent increments.

A. Fractional Brownian Motion

The ordinary Brownian motion $B(t)$ is a real random function with independent Gaussian increments, zero mean and standard deviation of the increment $B(t+\tau)-B(t)$ with $\tau > 0$ equal to $\tau^{1/2}$. If the intervals (t_1, t_2) and (t_3, t_4) do not overlap, the increment $B(t_2) - B(t_1)$ is independent of $B(t_4) - B(t_3)$.

The fractional Brownian motion $B_H(t)$ with parameter the Hurst exponent H with $0 < H < 1$ is defined by generalizing the ordinary Brownian motion as briefly summarized here below . Let $B(t)$ be the ordinary Brownian motion, then the Fractional Brownian Motion is a moving average of $dB(t)$ in which past increment of $B(t)$ are weighted by the kernel $(t-s)^\nu$ as follows:

$$B_H(t) = \frac{1}{\Gamma(\nu)}\Big\{ \int_{-\infty}^{0} [(t-s)^\nu - (-s)^\nu] dB(s) + \int_0^t (t-s)^\nu dB(s) \Big\} \quad (1)$$

and:

$$H = \nu + 1/2 \quad (2)$$

The exponent ν can take positive or negative values corresponding respectively to fractional integration or derivation of the Gaussian noise. If $\nu = 0$ then $H = 1/2$ and $B_{1/2}(t) = B(t)$. Compared to $B(t)$, the fractional Brownian motion with $0 < H < 1/2$ exhibits an amplification of the high-frequency components, leading to a overall antipersistent process. Conversely, the fractional Brownian motion with $1/2 < H < 1$ leads to an amplification of the low-frequency components compared to the ordinary Brownian motion, hence an overall persistent process is obtained.

The increments of the random function $B_H(t)$ are said to be self-affine with the exponent $H \geq 0$ if, for any $\lambda > 0$ and for any t_0:

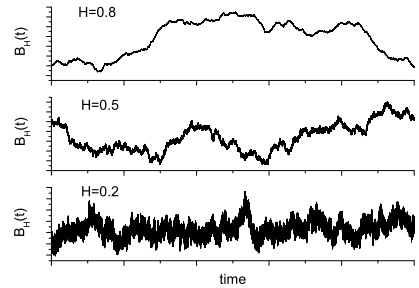

Fig. 1. Brownian motions respectively with $H = 0.2$, $H = 0.5$ and $H = 0.8$

$$B_H(t_0 + \lambda\tau) - B_H(t_0) \triangleq \lambda^H [B_H(t_0 + \tau) - B_H(t_0)] \quad (3)$$

where the notation $\triangleq$ means the same finite joint distribution functions. The variance of $B_H(t)$ obeys:

$$E[B_H(t+\tau) - B_H(t)]^2 \propto \tau^{2H} \quad (4)$$

and its standard deviation varies as τ^H.

B. Fractional Levy Motion

A stochastic process may satisfy the conditions to have self-affine and stationary increments without being Gaussian. In particular, by replacing $B(t)$ by a non-Gaussian process whose increments are stable random variables as defined by Levy, one obtains the fractional Levy-stable random functions with interdependent increments. The stable distributions are a generalization of widely used Gaussian distribution. Namely, stable distributions are the limits for the distributions of properly normalized sums of independent identically distributed random variables. Therefore these distributions, like the Gaussians, occur when the evolution of a system is the result of the sum of a large number of identical independent random factors. An important property of Levy probability distribution is the power law tails decreasing as $|x|^{-1-\alpha}$, $x \to \infty$, α is the Levy index, $0 < \alpha < 2$. Thus, the distribution moments of the order α diverge and the variance is non-finite. The other remarkable property of the Levy motions is their scale-invariance that makes them able to simulate fractal random processes. The Levy random processes are widely used in different areas, where the phenomena possessing scale invariance in a probabilistic sense are observed and in particular in economy, ecology, social sciences etc. Let $L_{\alpha,H}(t)$ indicate the process, whose increments are stably distributed with the Levy exponent α with $0 < \alpha < 2$. Similarly to the Fractional Brownian motion, the increments of a random function $L_{\alpha,H}(t)$ will be said to be self-affine with parameter H if for any $\lambda > 0$ and any t_0

$$L_{\alpha,H}(t_0 + \lambda\tau) - L_{\alpha,H}(t_0) \triangleq \lambda^H [L_{\alpha,H}(t_0 + \tau) - L_{\alpha,H}(t_0)] \quad (5)$$

The standard deviation of $L_{\alpha,H}$ obeys:

$$E[L_{\alpha,H}(t+\tau) - L_{\alpha,H}(t)]^2 \propto \tau^{2H} \quad (6)$$

and the parameter H is now defined as:

$$H = \nu + 1/\alpha \tag{7}$$

When $\alpha = 2$, the marginal distributions are Gaussian and the previous equations correspond to those of the fractional Brownian motions. The ordinary Brownian motion, i.e. $L_{\alpha,H}(t) \equiv B_{1/2}(t)$, is obtained when $\nu = 0$ and $\alpha = 2$. The fractional Brownian motion, $L_{\alpha,H}(t) \equiv B_H(t)$, is obtained with $\nu \neq 0$ and $\alpha = 2$. Furthermore, the ordinary Levy motion, $L_{\alpha,H}(t) \equiv L_H(t)$, is recovered with $\nu = 0$ and $H = 1/\alpha$. The fractional Levy motion can be thought of as the generalization of Fractional Brownian Motion, characterized by two parameters: the Hurst parameter H that measures the degree of the long-range dependence of the process and the Levy parameter α that measures the heaviness of the tails of the marginal distributions.

C. High-dimensional Fractals

The above described properties may be extended to random systems having an arbitrary dimension d. A fractal $B_H(r) : \mathbb{R}^d \to \mathbb{R}$, is characterized by:

$$E[B_H(r+\lambda) - B_H(r)]^2 \ \propto \|\lambda\|^\alpha \quad \text{with} \quad \alpha = 2H \ , \tag{8}$$

with $r = (x_1, x_2, ..., x_d)$, $\lambda = (\lambda_1, \lambda_2, ..., \lambda_d)$ and $\|\lambda\| = \sqrt{\lambda_1^2 + \lambda_2^2 + ... + \lambda_d^2}$.

The multifractional Brownian (MBM) and Levy motions (MFM) can de defined in any dimension as random processes which exhibit local self-similarity. This implies that the Hurst exponent is a time or space dependent variable rather than a constant.

III. Detrended Moving Average Algorithm

A number of fractal quantification methods, have been proposed to accomplish accurate and fast estimates of H in order to investigate correlations at different scales. This work is addressed to review an algorithm, called Detrending Moving Average (DMA), to estimate the Hurst exponent of fractals with arbitrary dimension [49]–[59]. The proposed method is based on a generalized variance of the fractional Brownian or Levy function around a moving average.

A. Detrending Moving Average Auto-Correlation [49]–[57]

To elucidate the way the Detrending Moving Average (DMA) algorithm works, in the following we consider its implementation for $d = 1$ and $d = 2$.

One-dimensional case:

$$\sigma^2_{DMA} = \frac{1}{N_1 - n_{1max}} \sum_{i_1=n_1-m_1}^{N_1-m_1} \left[f(i_1) - \tilde{f}_{n_1}(i_1) \right]^2 \ , \tag{9}$$

where N_1 is the length of the sequence, n_1 is the sliding window and $n_{1max} = \max\{n_1\} \ll N_1$. The quantity $m_1 = \text{int}(n_1\theta_1)$ is the integer part of $n_1\theta_1$ and θ_1 is a parameter ranging from 0 to 1. The relationship (9) defines a generalized variance of the sequence $f(i_1)$ with respect to the function $\widetilde{f}_{n_1}(i_1)$:

$$\widetilde{f}_{n_1}(i_1) = \frac{1}{n_1} \sum_{k_1=-m_1}^{n_1-1-m_1} f(i_1 - k_1) \ , \tag{10}$$

which is the moving average of $f(i_1)$ over each sliding window of length n_1. The moving average $\widetilde{f}_{n_1}(i_1)$ is calculated for different values of the window n_1, ranging from 2 to the maximum value n_{1max}. The variance σ^2_{DMA} is then calculated according to the Eq. (9) and plotted as a function of n_1 on log-log axes. The plot is a straight line, as expected for a power-law dependence of σ^2_{DMA} on n_1 [49], [55], [58]:

$$\sigma^2_{DMA} \sim n_1^{2H} \ . \tag{11}$$

Eq. (11) allows one to estimate the scaling exponent H of the series $f(i_1)$. Upon variation of the parameter θ_1 in the range $[0, 1]$, the index k_1 in $\widetilde{f}_{n_1}(i_1)$ is accordingly set within the window n_1. In particular, $\theta_1 = 0$ corresponds to average $f_{n_1}(i_1)$ over all the points to the left of i_1 within the window n_1; $\theta_1 = 1$ corresponds to average $f_{n_1}(i_1)$ over all the points to the right of i_1 within the window n_1; $\theta_1 = 1/2$ corresponds to average $f_{n_1}(i_1)$ with the reference point in the center of the window n_1.

Two-dimensional case [58]

For $d = 2$, the generalized variance defined by the Eq.(9) writes:

$$\sigma^2_{DMA} = \frac{1}{(N_1 - n_{1max})(N_2 - n_{2max})} \sum_{i_1=n_1-m_1}^{N_1-m_1} \sum_{i_2=n_2-m_2}^{N_2-m_2} \left[f(i_1, i_2) - \widetilde{f}_{n_1,n_2}(i_1, i_2) \right]^2 \tag{12}$$

with $\widetilde{f}_{n_1,n_2}(i_1, i_2)$ given by:

$$\widetilde{f}_{n_1,n_2}(i_1, i_2) = \frac{1}{n_1 n_2} \sum_{k_1=-m_1}^{n_1-1-m_1} \sum_{k_2=-m_2}^{n_2-1-m_2} f(i_1 - k_1, i_2 - k_2) \ . \tag{13}$$

The average $\widetilde{f}$ is calculated over sub-arrays with different size $n_1 \times n_2$. The next step is the calculation of the difference $f(i_1, i_2) - \widetilde{f}_{n_1,n_2}(i_1, i_2)$ for each sub-array $n_1 \times n_2$. A log-log plot of σ^2_{DMA}:

$$\sigma^2_{DMA} \sim \left[\sqrt{n_1^2 + n_2^2} \right]^{2H} \sim s^H \ . \tag{14}$$

as a function of $s = n_1^2 + n_2^2$, yields a straight line with slope H.

Depending upon the values of the parameters θ_1 and θ_2, entering the quantities $m_1 = \text{int}(n_1\theta_1)$ and $m_2 = \text{int}(n_2\theta_2)$ in the Eqs. (12,13), the position of (k_1, k_2) and (i_1, i_2) can be varied within each sub-array. (i_1, i_2) coincides with a vertex of the sub-array if: (*i*) $\theta_1 = 0$, $\theta_2 = 0$; (*ii*) $\theta_1 = 0$, $\theta_2 = 1$; (*iii*) $\theta_1 = 1$, $\theta_2 = 0$; (*iv*) $\theta_1 = 1$, $\theta_2 = 1$ (*directed implementation*). The choice $\theta_1 = \theta_2 = 1/2$ corresponds to take the point

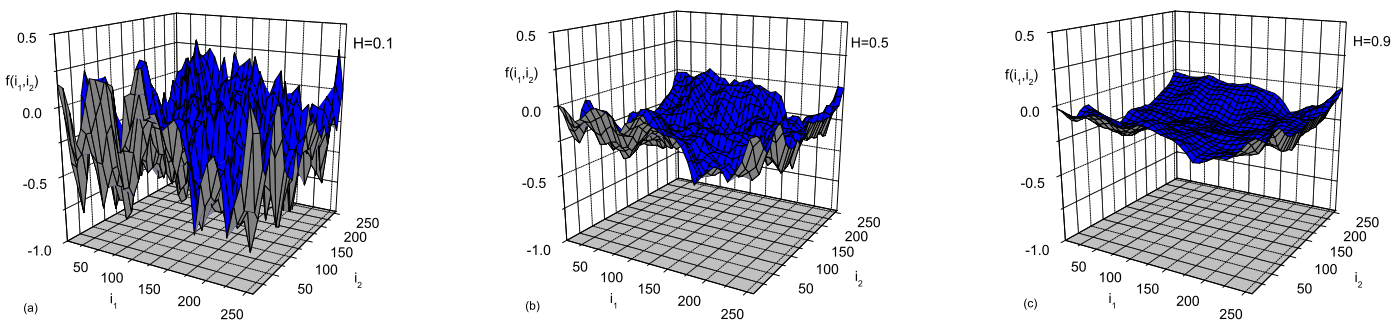

Fig. 2. Fractal Surfaces respectively with $H = 0.1$, $H = 0.5$ and $H = 0.9$.

(i_1, i_2) coinciding with the center of each sub-array $n_1 \times n_2$ (*isotropic implementation*) [60].

B. Detrending Moving Average Cross-correlation [59]

The *cross-correlation* C_{fg} of two nonstationary long-range correlated series $f(i_1)$ and $g(i_1)$ can be estimated by means of the following relationship:

$$C_{fg}(\tau) = \frac{1}{N_1 - n_{1max}} \sum_{i_1=n_1-m_1} [f(i)-\tilde{f}(i)][g^*(i+\tau)-\tilde{g}^*(t+\tau)] \tag{15}$$

where $\tilde{f}(i)$ and $\tilde{g}(i+\tau)$ indicate the moving averages means of $f(i)$ and $g(i+\tau)$. This relationship holds for space dependent sequences, as for example the chromosomes, by replacing time with space coordinate. Eq. (15) yields sound information provided the two quantities in square parentheses are jointly stationary and thus $C_{fg}(i, \tau) \equiv C_{fg}(\tau)$ is a function only of the lag τ.

IV. Examples

A. Volatility clustering and leverage effects

In this section, the Detrended Moving Average Algorithm is used for quantifying the long range correlation properties of the FIB30: the futures of the MIB30 index. In the Italian Stock Exchange -www.borsaitaliana.it- the MIBTEL index is built on all the traded stocks, while the MIB30 consider the thirty firms with higher capitalization and trading (the top 30 blue-chip index). The FIB30 is a future contract on the MIB30 index replaced in 2004 by the S&P MIB index. The objective of this operation was to obtain an increase in the transactions and in the efficiency of the stock market. We consider here the financial series of the FIB30 from June 1998 to June 2004 in order to exemplify some of the concepts and methods described in the previous sections. We consider here a tick-by-tick series sampled every minutes. Let $P(t)$ indicate the price of a stock. The fluctuations of $P(t)$ are expressed in terms of the returns:

$$r_\tau(t) = P(t+\tau) - P(t) \tag{16}$$

or alternatively in terms of the logarithmic returns:

$$r_\tau(t) = \ln P(t+\tau) - \ln P(t) \tag{17}$$

Another key quantity widely used in finance is the volatility. The explosive growth in derivative markets and the recent availability of high-frequency data have strongly highlighted its relevance. There are different definition of volatilities, here we refer to the following:

$$V_T(t) = \sqrt{\frac{1}{(T-1)} \sum_{t=1}^{T} \left[r(t) - \overline{r(t)}_T \right]^2} \tag{18}$$

where T is the volatility window.

It is a widely recognized *stylized fact* that volatility tends to cluster and exhibits positive persistence. The clustering of large moves and small moves in the price dynamics was documented by Mandelbrot and Fama and, then, confirmed by several other studies. The volatility clustering refers to the widely evidenced phenomenon that large changes in the price of a stock are often followed by other large changes, and small changes are followed by small changes. The practical consequence is that volatility shocks today are strongly correlated to the expectation of volatility in the future. The clustering of volatility has the consequence that a period of high volatility will eventually give rise to a period of low volatility and viceversa. This phenomenon is generally referred to as *mean reversion* and implies that there is an average level of the volatility to which the value will revert in the end.

Another *stylized fact* in finance is the *leverage effect* or volatility asymmetry. The fluctuations of return (i.e. the volatility) are related to whether returns are negative or positive. The leverage effect is a measure of the investor fear. Volatility rises when a stock's price drops and falls when the stock goes up. The impact of negative returns on volatility seems much stronger than the impact of positive returns (*down market effect*). To quantify the leverage effect and the down market effect, the cross correlation between returns and volatility of the price $P(t)$ should be quantified.

The Hurst exponents, calculated by the slope of the log-log plot of Eq. (9) as a function of n, are $H = 0.50$ (return) and $H = 0.6$ (volatility). Figs. 3 and 4 show the log-log plots of σ_{DMA} for the FIB30 returns and volatility. The scaling-law exhibited by the FIB30 series guarantees that its behavior is that of a fractional Brownian motion.

(a) (b) (c)

Fig. 4. FIB30 volatility, defined by Eq. (18), for (a) $T = 660\text{min}$ and (b) $T = 6600\text{min}$. The plot of the σ^2_{DMA} defined by Eq. (9) for the volatility series (a) and (b) are shown in (c). The lowest line in (c) is the DMA plot for an artificial Brownian motion with Hurst exponent $H = 0.6$. One can note deviations from the full fractal behavior at large scales, due to the finite size effects introduced by the volatility windows T.

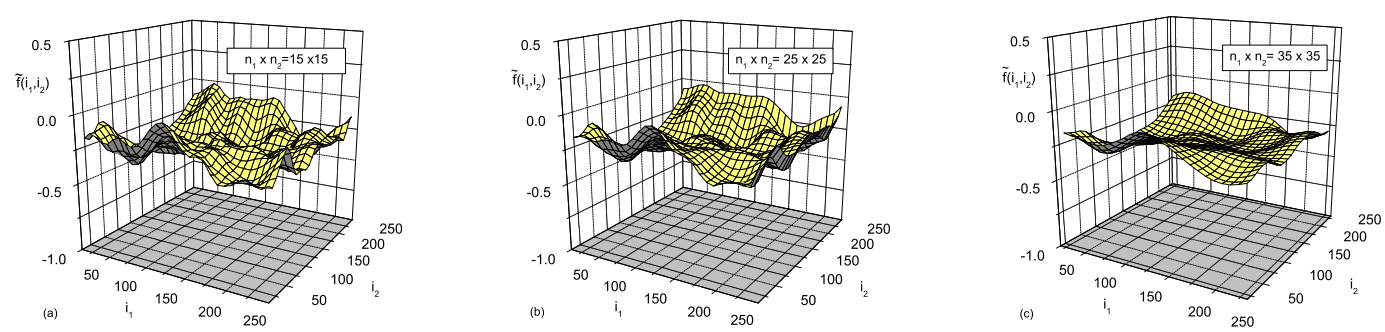

Fig. 5. Two-dimensional moving averages calculated by using Eq. (13) and the fractal surface with $H = 0.5$ shown in Fig. (2). The size $n_1 \times n_2$ refers to the local areas over which the 2D moving average is calculated.

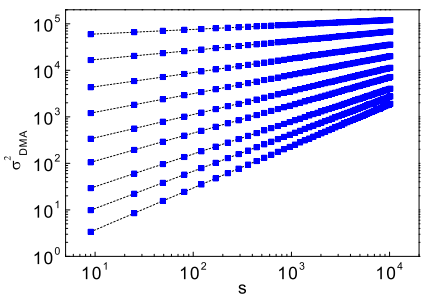

Fig. 6. Log-log plot of σ^2_{DMA} for fractal surfaces with size $N_1 \times N_2 = 4096 \times 4096$ and Hurst exponent H varying from 0.1 to 0.9 with step 0.1. The results correspond to the isotropic implementation of the Detrending Moving Average algorithm. Dashed lines represent linear fits.

B. Surface roughness

In this section, we discuss the implementation of the Detrending Moving Average Algorithm for estimating the Hurst exponent of fractal surfaces proposed in [58]. In Fig. 6, the log-log plots of σ^2_{DMA} as a function of s are shown for the synthetic fractal surfaces generated by the Cholesky-Levinson method. The surfaces have Hurst exponents ranging from 0.1 to 0.9 with step 0.1 and size $N_1 \times N_2 = 4096 \times 4096$. Dashed lines are the linear interpolation whose slope provide the Hurst exponent for each curve. The plots of σ^2_{DMA} as a function of s are in good agreement with the behavior expected on the basis of Eq. (14).

V. Conclusion

We have put forward an algorithm to estimate the Hurst exponent of fractals with arbitrary dimension, based on the high-dimensional generalized variance σ^2_{DMA} as defined by Eqs. (9) and (12). Other interesting applications that have been derived in the framework of this algorithm are the scaling properties of the clusters generated by the moving average and a measure of entropy for long range correlated series [52]–[54], [57].

References

[1] A. Carbone, G. Kaniadakis, and A.M. Scarfone, Eur. Phys. J. B **57**, 121 (2007).
[2] M. Batty, Environment and Planning A **37**, 1373 (2005).
[3] M.H.R. Stanley, L.A.N. Amaral, S.V. Buldyrev, S. Havlin, H. Leschhorn, P. Maass, M.A. Salinger, H.E. Stanley, 379, 804 (1996).
[4] H. Ebel, L.I. Mielsch, S. Bornholdt, Phys. Rev. E **66**, 035103 (2002).
[5] R. Pastor-Satorras, A. Vazquez, A. Vespignani, Phys. Rev. Lett. **87**, 258701 (2001).
[6] W. Willinger, R. Govindan, S. Jamin, V. Paxson, S. Shenker, Proc. Natl. Acad. Sci. **99**, 2573 (2002).
[7] S. Arianos, E. Bompard, A. Carbone and F. Xue, Chaos **19**, 013119 (2009).
[8] M. Batty, Nature **444**, 592 (2006).
[9] A. Blank, S. Solomon, Physica A **287**, 279 (2000).
[10] G. Caldarelli, R. Marchetti, L. Pietronero, Europhys. Lett. **52**, 386 (2000).
[11] S.N. Dorogovtsev, A.V. Goltsev, J.F.F. Mendes, Phys. Rev. E **65**, 066122 (2002).
[12] C.M. Song, S. Havlin, H.A. Makse, Nature **433**, 392 (2005).
[13] E. Ravasz, A.L. Barabási, Phys. Rev. E **67**, 026112 (2003).
[14] A. Carbone, G. Kaniadakis and A.M. Scarfone, Physica A **382**, xi-xiv (2007).
[15] V. Alfi, F. Coccetti, A. Petri, L. Pietronero, Eur. Phys. J. B **55**, 135 (2007).
[16] M. Bartolozzi, C. Mellen, T. Di Matteo, T. Aste Eur.Phys. J. B **58**, 207 (2007).
[17] T. Di Matteo, T. Aste, M.M. Dacorogna, J. Bank. & Fin. **29**, 827 (2005).
[18] M. Couillard, M. Davison, Physica A **348**, 404 (2005).
[19] L. Calvet, A. Fisher, Review of Economics and Statistics **84**, 381 (2002).
[20] J.P. Bouchaud, M. Potters, M. Meyer, Eur. Phys. J. B **13**, 595 (2000).
[21] J. Feigenbaum, Rep. Prog. Phys. **66**, 1611 (2003).
[22] T. Lux, Int. J. of Mod. Phys. C **15**, 481 (2004).
[23] W.B. Wu, G. Michailidis and D. Zhang, IEEE Transactions on Information Theory **50**, 1086 (2004).
[24] W.B. Wu and Z. Zhao, J. of the Royal Stat. Soc. Series B. **69**, 391 (2007).
[25] A. Karasaridis, D. Hatzinakos, IEEE Trans. Commun. **49**, 1203 (2001).
[26] S. Thurner, M.C. Feurstein, and M.C. Teich, Phys. Rev. Lett. **80**, 1544 (1998).
[27] A.L. Goldberger et al. Proc. Natl. Acad. Sci. **99**, 2466 (2002).
[28] C.K. Peng, S.V. Buldyrev, S. Havlin, M. Simons, H.E. Stanley, and A.L. Goldberger, Phys. Rev. E **49**, 1685 (1994).
[29] Y. Ashkenazy, D. Baker, H. Gildor, S. Havlin, Geophys. Res. Lett. **30**, 2146 (2003).
[30] P. Huybers, W. Curry, Nature **441**, 7091 (2006).
[31] D.L. Blair and A. Kudrolli, Phys. Rev. Lett. **94**, 166107 (2005).
[32] L. Ponson, D. Bonamy, and E. Bouchaud, Phys. Rev. Lett. **96**, 035506 (2006).
[33] A. Hansen, G.G. Batrouni, T. Ramstad and J. Schmittbuhl, Phys. Rev. E **75**, 030102(R) (2007).
[34] E. Bouchbinder, I. Procaccia, S. Santucci, and L. Vionel, Phys. Rev. Lett. **96**, 055509 (2006).
[35] J. Schmittbuhl, F. Renard, J.P. Gratier, and R. Toussaint, Phys. Rev. Lett. **93**, 238501 (2004).
[36] S. Santucci, K.J. Maloy, A. Delaplace, et al. , Phys. Rev. E **75**, 016104 (2007).
[37] J.B. Sokoloff, Phys. Rev. E **73**, 016104 (2006).
[38] P. Levitz, D.S. Grebenkov, M. Zinsmeister, K.M. Kolwankar and B. Sapoval, Phys. Rev. Lett., **96**, 180601 (2006).
[39] K. Malek and M.O. Coppens, Phys. Rev. Lett. **87**, 125505 (2001).
[40] E.N. Oskoee and M. Sahimi, Phys. Rev. B **74**, 045413 (2006).
[41] M. Filoche and B. Sapoval, Phys. Rev. Lett. **84**, 5776 (2000).
[42] D.R. Vollet, D.A. Donati, A. Ibanez Ruiz, and F.R. Gatto, Phys. Rev. B **74**, 024208 (2006).
[43] B. Suki, A.L. Barabasi, Z. Hantos, F. Petak, and H.E. Stanley, Nature **368**, 615 (1994).
[44] C. Yang, U. Tartaglino and B.N.J. Person, Phys. Rev. Lett. **97**, 16103 (2006).
[45] A. Mihranyan, M. Stromme, Surf. Sc. **601**, 315 (2007).
[46] P.E. Fisher and N.J. Tate, Prog. in Phys. Geography **30**, 467 (2006).
[47] A.K. Sultan-Salem, G.L. Tyler, J. of Geophys. Res.-Planets **111**, E06S07 (2006).
[48] B.B. Mandelbrot and J.W. Van Ness, SIAM Rev. **4**, 422 (1968).
[49] E. Alessio, A. Carbone, G. Castelli, and V. Frappietro, Eur. Phys. Jour. B **27**, 197 (2002).
[50] A. Carbone and G. Castelli, Noise in Complex Systems and Stochastic Dynamics, L. Schimansky-Geier, D. Abbott, A. Neiman, C. Van den Broeck, Eds., Proc. of SPIE, **407**, 5114 (2003).
[51] A. Carbone, G. Castelli and H.E. Stanley, Phys. Rev. E **69**, 026105 (2004).
[52] A. Carbone and H.E. Stanley, Physica A **340**, 544 (2004).
[53] A. Carbone, G. Castelli and H.E. Stanley, Physica A **344**, 267 (2004).
[54] A. Carbone and H.E. Stanley, Noise in Complex Systems and Stochastic Dynamics, (Eds. Z. Gingl, J.M. Sancho, L. Schimansky-Geier, J. Kertesz) Proc. of SPIE **5471**, 1 (2004).
[55] S. Arianos and A. Carbone, Physica A **382**, 9 (2007).
[56] L. Xu et al. Phys. Rev. E **71**, 051101 (2005).
[57] A. Carbone and H.E. Stanley, Physica A **384**, 21 (2007).
[58] A. Carbone, Phys. Rev. E **76**, 056703 (2007).
[59] S. Arianos and A. Carbone, J. Stat. Mech: Theory and Experiment P03037, (2009).
[60] Source and executable files of the DMA algorithm can be downloaded at www.polito.it/noiselab/utilities.